J Mater Sci (2007) 42:444–464
DOI 10.1007/s10853-006-0874-1

The hydration of slag, part 2: reaction models for blended cement

W. Chen · H. J. H. Brouwers

Received: 10 February 2005 / Accepted: 22 December 2005 / Published online: 18 November 2006

Abstract The hydration of slag-blended cement is studied by considering the interaction between the hydrations of slag and Portland cement clinker. Three reaction models for the slag-blended cement are developed based on stoichiometric calculations. These models correlate the compositions of the unhydrated slag-blended cement with the quantities and compositions of the hydration products. The model predictions are further used to calculate some properties of hydrating slag cement pastes, including the molar fractions of products, the water retention, chemical shrinkage and porosities of pastes. The models are validated by comparing the model predictions with the measurements and proven to be successful in quantifying the hydration products, predicting the composition of the main hydration product (C-S-H) and calculating the properties of the hydration process. The model predictions show that as the slag proportions in the blended cement changes, water retention in the hydration products changes only slightly if compared to that of Portland cement, but the chemical shrinkage can vary in a wide range, depending on the slag hydration degree in the cement.

List of symbols

Oxides

A	Al_2O_3
S	SiO_2
C	CaO
F	Fe_2O_3
M	MgO
$\bar{S}$	SO_3
H	H_2O

Roman

AEM	Analytical electron microscopy
A/S	A/S molar ratio in C-S-H
C/S	C/S molar ratio in C-S-H
$\overline{C/S}$	Equilibrated C/S molar ratio in C-S-H
EDX	Energy dispersive X-ray
EMPA	Electron microprobe analysis
GGBFS	Ground granulated blast-furnace slag
M	Molar mass of substance [g/mol]
NMR	Nuclear magnetic resonance
SEM	Scanning electron microscopic
TEM	Transmission electron microscopy
TG	Thermogravimetry
XRD	X-ray diffraction
w/c	water/cement ratio of paste
m	Mass of substance
n	Moles of substance
n_H^t	Total moles of water retained in products
p	Proportion of the CH consumed to that produced
x	Mass fraction of constituent in slag and Portland cement
y	Mole content of constituent in slag and Portland cement [mol/g]

Greek

Φ	Porosity
Ψ	Chemical shrinkage
γ	Relative hydration degree of slag
λ	Slag proportion in the blended cement

W. Chen · H. J. H. Brouwers (✉)
Faculty of Engineering Technology, Department of Civil Engineering, University of Twente, P.O. Box 217, Enschede 7500 AE, The Netherlands
e-mail: h.j.h.brouwers@ctw.utwente.nl

λ^0	Transitional slag proportion
ρ	Density [g/cm^3]
ω	Molar volume [cm^3/mol]

Superscript

c	Product consumed by slag hydration
p	Product of Portland cement hydration
r	Reacted slag
ur	Unreacted slag

Subscript

AH	Tetracalcium aluminate hydrate
AFt	Ettringite
C-S-H	Calcium silicate hydrate
CH	Portlandite
HG	Hydrogarnet
HT	Hydrotalcite
H	Water retained in hydration product
c	Blended cement
cp	Capillary porosity
gp	Gel porosity
gyp	Gypsum
hp	Hydration product
hcp	Hydrating cement paste
monoc	Monocarbonate
new	Non-evaporable water
p	Portland cement
sl	Slag
w	Water
x	H/S ratio in C-S-H

Introduction

The granulated blastfurnace slag is commonly blended with (ordinary) Portland cement or clinker to produce slag-blended cement after being ground to the fineness comparable to Portland cement. The two ingredients (Portland cement and slag) hydrate at different rates. After being mixed with water, Portland cement in the blended cement starts to hydrate immediately. Meanwhile, a small amount of GGBFS reacts [1], probably due to the presence of gypsum in cement. Then, the hydration of slag is greatly activated by alkalis and later by the Portlandite (CH, cement notation is used, C = CaO, S = SiO_2, A = Al_2O_3, M = MgO, $\bar{S}$ = SO_3, H = H_2O) released by the hydration of Portland cement. Generally, the slag hydration rate is far lower than that of clinker. After one year, about 90%–100% of the clinker has hydrated in the blended cement paste [2]. At the same age, only about 50%–70% of the slag has hydrated [3–6].

The main hydration products of pure slags comprise C-S-H, hydrotalcite, an iron-containing hydrogarnet, ettringite and some AFm phases [7]. The composition of hydrotalcite is related to the natural mineral $M_6A\bar{C}H_{12}$. But the M/A ratio in the slag hydration product is not fixed to six and differs over a wide range [8]. Pure phase hydrotalcite is difficult to distinguish in the hardened cement paste because it is closely mixed with C-S-H. In this study, the formula M_5AH_{13} is used, following the same reasons as in Part 1 of this research [7]. AFm phases, including the tetracalcium aluminate hydrate (C_4AH_{13}) and strätlingite (C_2ASH_8) are found in the hydration products of pure slag. But, their formations highly depend on the oxide composition of slag, as revealed in Part 1 of this research [7]. If the aluminum content in slag is relatively low or the magnesium content is high, the AFm phases are not formed.

The main hydration products of Portland cement include C-S-H, CH, C_4AH_{13}, ettringite, hydrogarnet and monosulfate [8]. Monosulfate is more likely replaced by ettringite and hemi/monocarbonate because even a small amount of carbon dioxide is sufficient to carbonate the former into the latter.

Hydration products in the slag-blended cement paste comprise those products from both Portland cement and slag hydrations except that the amount of CH formed by the Portland cement hydration is influenced by the slag hydration [9–11]. C-S-H is the most abundant product in blended cement pastes. Its C/S ratio (in moles) is generally lower than that in the Portland cement paste. However, the C/S ratio in C-S-H is still higher than the C/S ratio in the pure slag (about 1.0–1.1), indicating additional calcium demand by the slag hydration. This calcium demand is supplied either by the CH formed by the Portland cement hydration [12], or by the lower C/S ratio in the C-S-H [13]. In this respect, the CH produced by the hydration of Portland cement acts as not only an activator or catalyst to the slag hydration, but also as a reactant.

Richardson and Groves [10] studied the microstructure and composition of a group of slag-blended cement pastes with various blend proportions using transmission electron microscopy (TEM) with microanalysis combined with the electron microprobe analysis (EMPA). In the 3-year-old paste, no significant difference was found among the C/S and A/S ratios in the C-S-H gels in the inner products of both calcium silicates and slag and all the outer products. Duchesne and Bérubé [14] also found this unimodel distribution of compositions in the hydration products in the 3-year-old specimens containing different supplementary cementitious materials. The unimodel of composition distribution in C-S-H is in line with the observations in

the old tricalcium silicate pastes and Portland cement pastes in which a compositional equilibrium of C-S-H in the inner and outer products was attained [10, 15]. Conclusion can be drawn based on this unimodel distribution that the C-S-H from both the Portland cement and slag hydrations has the same compositions.

Summarizing, the hydration products present in the hydrating slag-blended cement paste include C-S-H, M_5AH_{13}, $C_6A\bar{S}_3H_{32}$, CH and C_4AH_{13}. The Fe-containing hydrogarnet and other products are not considered due to their trace levels. According to the model predictions in Part 1, either C_4AH_{13} or strätlingite exists in minor amounts. C_4AH_{13} is taken instead of the strätlingite in the slag hydration products because the latter is incompatible with CH, one of the main hydration products of Portland cement [16]. Note that the water content in these hydration products might vary in different hydration states, which are defined as the drying conditions that these products are subject to.

In the existing researches efforts have been made to model the hydration of slags by using stoichiometry calculations. Taylor [8] proposed a method for calculating the quantity of hydration product of slag. All the magnesium was assumed to enter the hydrotalcite and silicon to enter C-S-H. For facilitating this calculation, the C/S and A/C ratios in C-S-H were assumed beforehand to be 1.55 and 0.045, respectively. Richardson et al. [17] investigated the stoichiometry of the reaction between slag and CH. Both the compositions of the hydration products and the consumption data of slag and CH were measured by using TGA, scanning electron microscopy (SEM) and X-ray diffraction (XRD). Based on the compositions of the hydration products, the molar ratio between the reacted slag and CH were derived by using a molar balance calculation. The obtained molar ratios were compared to the measured data. An estimated hydration stoichiometry ratio (2.6 mol of CH consumed by each mole of slag reacted) was proposed. The C/S ratio in C-S-H was set beforehand to a value of 1.42.

However, the predetermination of C/S and A/C (or A/S) ratios in C-S-H, as used in aforesaid researches, is only applicable for particular slag proportions in the blended cement. Richardson and Groves [10] found that the composition of C-S-H is clearly influenced by the slag proportions in the blended cement. They found that increasing slag proportions resulted in decreasing C/S ratios and increasing A/S ratios in C-S-H. Therefore, the stoichiometry proposed by Taylor [8] and Richardson et al. [17] is only applicable to some specific slag/clinker or slag/CH ratios, for example, 80% slag/20% CH (m/m) as used in the research of Richardson et al. [17].

Modeling the hydration of the slag-blended cement is important for better understanding the chemistry underlying and for simulating its microstructure. Outputs of the models can be used for further purpose, such as evaluating the durability of concrete, predicting strength and modeling the chemical composition of the liquid phase in concrete. Although there are some studies aiming to reveal the interaction between slag and pure CH, to the authors' knowledge, no studies are available on the overall hydration of slag-blended cement considering their interactions. In this study, three general reaction models for slag-blended cement are proposed based on stoichiometry calculations. They correlate the compositions of the unhydrated slag-blended cement (the mineral compositions of the slag and Portland cement and the blending proportions) with the quantities and compositions of the hydration products. Mutual influence between the hydration of the two types of binders (slag and Portland cement) is investigated. The different hydration rates between the slag and Portland cement are accounted for.

The stoichiometric models are further used to predict some specific characteristics of hydrating slag cement pastes, including the molar fraction of products, water retention, chemical shrinkage and porosities of the pastes. These properties are either difficult to measure in practice, or available in experiments for validating the models. The models are validated with measurements in a serial of experiments investigating slag-blended cements with various ingredients. The model predictions are compared to the measured data and good agreements are observed.

Stoichiometric models for slag cement hydration

Stoichiometric models for slag cement hydration are developed with the oxide compositions of the starting materials and their proportions in the mix. The hydration of the two constituents (slag and Portland cement) is first investigated separately, although they are homogeneously mixed in the cement and interact with each other. Then, models are established considering the interaction of their hydration products.

Reaction model for pure slag

For the slag in the blended cement, the masses and moles of oxides in the slag can be calculated by the following equations:

$$m_i = m_{sl} \cdot x_{i,sl} \tag{1}$$

$$n_i = m_i/M_i = m_{sl} \cdot x_{i,sl}/M_i = m_{sl} \cdot y_{i,sl} \tag{2}$$

in which m_{sl} is the mass of slag in the cement; i is the main oxide in the slag (C, S, A, M, or $\bar{S}$, respectively), m_i and n_i are the mass and mole of the phase i, respectively; $x_{i,sl}$ and M_i are the mass fraction and molar mass of oxide i in the slag, respectively; $y_{i,sl}$ is the molar content of oxide i in the slag (mol/g slag), which is calculated from $x_{i,sl}$ and M_i.

As discussed in the previous section, the main hydration products of slag include C-S-H, M_5AH_{13}, $C_6A\bar{S}_3H_{32}$, and C_4AH_{13}. Formation of strätlingite is not considered. Here, only five oxides, namely C, S, A, M and $\bar{S}$, are selected among the oxides constitutions of slag because they are the most abundant oxides in the slag and are combined in the selected products. Since all the magnesium from slag reacts into the hydrotalcite, moles of hydrotalcite are readily calculated as:

$$n_{HT} = n_M/5 \tag{3}$$

in which n_M follows from Eq. (2). Similarly, the moles of $C_6A\bar{S}_3H_{32}$ are calculated from the $\bar{S}$ content in the slag as:

$$n_{AFt} = n_{\bar{S}}/3 \tag{4}$$

in which $n_{\bar{S}}$ follows from Eq. (2). The calculation above shows that part of the C and A in the slag is firstly combined with M and $\bar{S}$ to form the hydrotalcite and ettringite. The moles of C and A remaining for the other hydration products now read:

$$n_C^* = n_C - 6n_{AFt} = m_{sl} \cdot (y_{C,sl} - 2y_{\bar{S},sl}) = m_{sl} \cdot y_C^* \tag{5}$$

$$\begin{aligned} n_A^* &= n_A - n_{HT} - n_{AFt} \\ &= m_{sl} \cdot (y_{A,sl} - y_{M,sl}/5 - y_{\bar{S},sl}/3) \end{aligned} \tag{6}$$

in which Eqs. (3) and (4) are already substituted. In fact, y_C^* and y_A^* in Eqs. (5) and (6) are equivalent to the quantity of C and A remaining for the other hydration products per unit mass of slag, respectively.

Substitution of S by A in the bridging tetrahedral of a dreierkette structure in C-S-H, the main hydration product of slag, was observed in experiments [18, 19]. The substitution is even more prominent for C-S-H with low C/S ratios, which applies in the C-S-H formed by the slag hydration. In Part 1 of this research, a large part of A in the slag was found to enter the hydration product C-S-H and to substitute for S [7]. Therefore, the A substitution in the C-S-H is important for modeling the hydration and is also considered in this study.

However, the degree of A substitution in the C-S-H is limited. Taylor [20] concluded that the maximum degree of A substitution in C-S-H formed by the hydration of Portland cement or C_3S corresponds to an A/C ratio of 0.01. Later, Chen and Brouwers [7] proposed that the maximum degree of A substitution is related to the S/C ratio in C-S-H by the relation proposed by Richardson [18] as:

$$S/C = 0.4277 + 4.732\ A/C \tag{7}$$

If the maximum degree of substitution in C-S-H is achieved, they assumed that the remaining A is combined with C to form C_4AH_{13}. The formation of C_4AH_{13} thus highly depends on the amount of the A in the slag. C_4AH_{13} is formed if the quantity of A in the slag is adequate for the formation of ettringite and hydrotalcite and for the maximum degree of substitution in C-S-H. The hydration equation of slag is thus summarized as:

$$C_{n_C^*}S_{n_S}A_{n_A^*} + n_H H \rightarrow n_S C_{(C/S)}SA_{(A/S)}H_x \tag{8}$$

in which n_H is the quantity of water retained by hydration products; x is the H/S ratio in C-S-H. Note that in the hydration equation (4), hydrotalcite and ettringite are not included because their quantities are readily calculated using the moles of M and $\bar{S}$ in slag using Eqs. (3) and (4). The oxides M and $\bar{S}$ (constituents always reacting to form the hydrotalcite and ettringite) are not included in the starting material, either. If C_4AH_{13} is formed, the hydration equation of slag turns into:

$$C_{n_C^*}S_{n_S}A_{n_A^*} + n_H H \rightarrow n_S C_{(C/S)}SA_{(A/S)}H_x + n_{AH,sl}C_4AH_{13} \tag{9}$$

in which $n_{AH,sl}$ is the quantity of C_4AH_{13}.

Reaction model for calcium silicates in Portland cement clinker

The exchange of CH formed by the hydrations of calcium silicates with the slag hydration is important for modeling the slag cement hydration. Since the calcium silicates are the most abundant constituents in Portland cement, only the hydrations of calcium silicates in Portland cement are coupled with the slag hydration. CH produced by their hydrations is considered to be available for the slag hydration. Furthermore, since

most reaction models available for Portland cement hydration are based on the hydration of the individual clinker phases [8, 21–25], the hydrations of calcium silicates are assumed not to interact with the hydration of the other clinker phases (aluminate and ferrite) in Portland cement.

The phase composition of Portland cement can be calculated quantitatively from its oxide composition by using Bogue's equations or measured experimentally by using techniques such as QXRD, microscopy and liquid extraction. The masses and moles of C_3S, C_2S, C_3A and C_4AF in Portland cement are calculated from the mass of Portland cement in the blended cement as:

$$m_i = m_p \cdot x_i \tag{10}$$

$$n_i = \frac{m_i}{M_i} = \frac{m_p \cdot x_i}{M_i} \cdot = m_p \cdot y_i \tag{11}$$

in which m_p is the mass of Portland cement; i is the clinker phase in Portland cement; m_i and n_i are the mass and mole of phase i, respectively; x_i is the mass fraction of phase i in Portland cement; M_i is the molar mass of phase i (g/mol); y_i is the molar content of phase i in Portland cement (mol/g Portland cement) calculated with x_i and M_i.

The hydration equations of C_3S and C_2S are summarized as:

$$C_3S + (1.2 + x)H \rightarrow C_{1.8}SH_x + 1.2CH \tag{12}$$

$$C_2S + (0.2 + x)H \rightarrow C_{1.8}SH_x + 0.2CH \tag{13}$$

In Eqs. (12) and (13), the C/S ratio in C-S-H equals to 1.8, which is commonly observed in experiments [10] and generally used in cement chemistry. Note that the C/S ratio used here (1.8) is considered to be the highest C/S ratio in C-S-H from the slag-blended cement in the following discussions because blending slag with Portland cement was found to lower the C/S ratio in the hydration product C-S-H [10]. The quantities of CH and C-S-H from the calcium silicate reactions are calculated with Eqs. (12) and (13) as:

$$n^p_{CH} = 1.2 \cdot n_{C_3S} + 0.2 \cdot n_{C_2S} = m_p \cdot (1.2y_{C_3S} + 0.2y_{C_2S}) \tag{14}$$

$$n^p_{C-S-H} = n_{C_3S} + n_{C_2S} = m_p \cdot (y_{C_3S} + y_{C_2S}) \tag{15}$$

Reactions of the four clinker phases are treated independently. The calcium silicates react to form CH and C-S-H. The A substitution is not considered in C-S-H formed by the hydration of calcium silicate.

Modeling the interaction between the hydrations of slag and calcium silicates is possible by using their hydration equations. In the following discussion, three reaction models are proposed for the hydration of slag-blended cement considering different degree of interaction between the slag and clinker hydrations.

Reaction models for the slag-blended cement

Based on the masses of slag (m_{sl}) and Portland cement (m_p) in the blended cement, the total mass reads:

$$m = m_{sl} + m_p \tag{16}$$

The slag proportion (mass fraction of slag in the blended cement, namely λ) is defined as:

$$\lambda = \frac{m_{sl}}{m} = \frac{m_{sl}}{m_{sl} + m_p} \tag{17}$$

The masses of slag and Portland cement in the blended cement thus read:

$$m_{sl} = m \cdot \lambda; \quad m_p = m \cdot (1 - \lambda) \tag{18}$$

If $\lambda = 0$ the cement is apparently pure Portland cement and if $\lambda = 1$ the cement is pure slag, which exhibits very weak hydraulic capability without alkali activation.

For modeling the hydration of slag-blended cement, the hydration degrees of slag and clinker at a certain age are important. As observed in experiments, the slag and clinker in the blended cement paste hydrate at different rates. Their hydration degrees depend on many factors such as the water/cement (w/c) ratio, temperature, reactivity of slag and the fineness of components, and thus are difficult to predict. However, for predicting the stoichiometry of the hydration reaction, the relative hydration degree is necessary. It physically represents the ratio of the slag hydration degree to that of clinker. If the actual degree of clinker hydration is known, the slag hydration degree can be calculated by using the relative hydration degree. The actual degree of clinker hydration can be predicted by using empirical equations or numerical models. For simplicity, in this study the clinker is assumed to hydrate completely, corresponding to a curing age of about one year. At this age, only part of the slag in the blended cement hydrates, for example, about 50%–70% in the studies of Luke and Glasser [3], Battagin [4] and Lumley et al. [6]. Hence, with this assumption, the relative hydration degree equals to the degree of slag hydration. The mass of hydrated slag is thus calculated as:

$$m_{sl}^{r} = \gamma \cdot m_{sl} \tag{19}$$

in which γ is the slag hydration degree, m_{sl}^{r} and m_{sl} are the masses of the hydrated and initial slag, respectively. Hereafter m_{sl}^{r} is used instead of the mass of the initial slag when calculating the moles of oxides from the hydrated slag.

Studies have shown that the amount of CH in the hardened blended cement pastes decreased with increasing slag proportions in blended cement [16]. It was even not detected if the slag proportion in the blended cement was high, indicating a complete consumption of CH by the slag hydration [9–12, 16]. Therefore, to consider the consumption of CH by the slag hydration is important for modeling the hydration of slag-blended cement. The moles of CH involved the slag hydration, namely n_{CH}^{c}, can be the partial or total amount of CH produced by the clinker hydration. The hydration equation of the slag including this part of CH is thus written from Eq. (8) as:

$$C_{n_C^*}S_{n_S}A_{n_A^*} + n_{CH}^{c}CH + n_H H \rightarrow n_S C_{(C/S)_{sl}}SA_{(A/S)}H_x \tag{20}$$

in which n_C^* and n_A^* are the quantities of C and A in the slag remaining for the C-S-H (see discussion in previous section). A molar balance calculation between the two sides of Eq. (20) yields C/S and A/S ratios in C-S-H as:

$$(C/S)_{sl} = (n_C^* + n_{CH}^{c})/n_S \tag{21}$$

$$A/S = n_A^*/n_S \tag{22}$$

If the blended cement is pure slag ($\lambda = 1$), no clinker exists in the cement and $n_{CH}^{c} = 0$. Equation (20) is further coupled with the hydration equations of calcium silicates (Eqs. (12) and (13)) to yield a final equation as:

$$\begin{aligned} n_{C_3S}C_3S + n_{C_2S}C_2S + C_{n_C^*}S_{n_S}A_{n_A^*} + n_H^{t}H \rightarrow \\ (n_{C_3S} + n_{C_2S})C_{1.8}SH_x + (n_{CH}^{p} - n_{CH}^{c})CH \\ + n_S C_{(C/S)_{sl}}SA_{(A/S)}H_x \end{aligned} \tag{23}$$

in which n_H^{t} is the mole of retained water in the hydration product. This amount of water equals to the amount of needed water for the hydration of blended cement. In this study, the C/S ratios are averaged to an equilibrated value, namely $\overline{C/S}$, because of the compositional equilibrium in C-S-H from both Portland cement and slag hydrations. Hence, Eq. (23) is rewritten as:

$$\begin{aligned} n_{C_3S}C_3S + n_{C_2S}C_2S + C_{n_C^*}S_{n_S}A_{n_A^*} + n_H^{t}H \rightarrow \\ (n_{C_3S} + n_{C_2S})C_{(\overline{C/S})}SH_x + n_S C_{(\overline{C/S})}SA_{(A/S)}H_x \\ + (n_{CH}^{p} - n_{CH}^{c})CH \end{aligned} \tag{24}$$

Note that in the hydration equation (24), distinction is made between the C-S-H from the clinker and slag hydrations because A in slag is considered to be only available for substitution in C-S-H from the slag hydration. The $\overline{C/S}$ of C-S-H is calculated by using the molar balance as:

$$\begin{aligned} \overline{C/S} &= \frac{3n_{C_3S} + 2n_{C_2S} + n_C^* - n_{CH}^{p} + n_{CH}^{c}}{n_{C_3S} + n_{C_2S} + n_S} \\ &= \frac{1.8(n_{C_3S} + n_{C_2S}) + n_C^* + n_{CH}^{c}}{n_{C_3S} + n_{C_2S} + n_S} \end{aligned} \tag{25}$$

in which Eq. (14) is already substituted. The A/S ratio in C-S-H is calculated using Eq. (22).

Furthermore, for some slags and slag proportions, there is adequate A to enter the C-S-H and the maximum substitution degree for S is achieved and another equation for determining $\overline{C/S}$ needs to be derived. In this case, based on Eq. (7), the $\overline{C/S}$ and A/S ratios in C-S-H fit into:

$$A/S = (1 - 0.4277 \cdot \overline{C/S})/4.732 \tag{26}$$

The remaining A will be combined with C to form C_4AH_{13}. The quantity of remaining A reads:

$$n_{A,AH} = n_A^* - n_S \cdot (A/S) = n_A^* - n_S \cdot (1 - 0.4277\,\overline{C/S})/4.732 \tag{27}$$

So, the moles of C_4AH_{13} are equal to those of the available A ($n_{AH,sl} = n_{A,AH}$) based on its stoichiometry. Now using the molar balance of C between the starting material and the hydration products, the C/S ratio in the C-S-H is calculated as:

$$\begin{aligned} \overline{C/S} &= \frac{3n_{C_3S} + 2n_{C_2S} + n_C^* - n_{CH}^{p} + n_{CH}^{c} - 4n_{AH,sl}}{n_{C_3S} + n_{C_2S} + n_S} \\ &= \frac{1.8(n_{C_3S} + n_{C_2S}) + n_C^* + n_{CH}^{c} - 4n_{AH,sl}}{n_{C_3S} + n_{C_2S} + n_S} \end{aligned} \tag{28}$$

in which Eq. (14) is already substituted. Substituting Eq. (27) into (28) and solving the equation gives:

$$\overline{C/S} = \frac{1.8(n_{C_3S} + n_{C_2S}) + n_C^* + n_{CH}^{c} + 0.85n_S - 4n_A^*}{1.36n_S + n_{C_3S} + n_{C_2S}} \tag{29}$$

With the C/S ratio in Eq. (29), the A/S ratio and the quantity of C_4AH_{13} are calculated using Eqs. (26) and (27).

The C/S ratio in C-S-H is lower than that in pure Portland cement because blending the slag (which has a lower C/S ratio) with Portland cement clearly lowers the C/S ratio in C-S-H. Therefore, it holds that:

$$\overline{C/S} \leq 1.8 \tag{30}$$

In the case that there is no adequate A in the slag, C_4AH_{13} is not formed and C/S ratio follows from Eq. (25). Now substituting Eq. (25) into inequality (30) gives:

$$n_{CH}^{c} \leq 1.8n_S - n_C^* \tag{31}$$

and in the other case that there is adequate A in the slag, C_4AH_{13} is formed and the C/S ratio follows from Eq. (29). Again substituting Eq. (29) into inequality (30) and rewriting it gives:

$$n_{CH}^{c} \leq 1.8n_S - n_C^* + 4n_{AH,sl} \tag{32}$$

In Eqs. (25) and (29), the $\overline{C/S}$ in the hydration product C-S-H varies with the quantity of CH consumed by the slag hydration. Hence, three reaction models are put forward depending on the amount of CH entering the slag hydration.

Model 1: No CH enters the C-S-H formed by the slag hydration

In this model, no CH produced by the hydration of the calcium silicates is available for the hydration of slag, indicating $n_{CH}^{c} = 0$. Only the C-S-H from the slag and the clinker hydrations interact with each other to obtain a compositional equilibrium.

Two cases are again distinguished, corresponding to the formation of C_4AH_{13} or not. In Case 1, in which there is no adequate A in the slag to reach the maximum substitution degree for S in C-S-H, C_4AH_{13} is not formed. According to Eq. (25) and because $n_{CH}^{c} = 0$, the C/S ratio in C-S-H reads:

$$\overline{C/S} = \frac{1.8(n_{C_3S} + n_{C_2S}) + n_C^*}{n_{C_3S} + n_{C_2S} + n_S} \tag{33}$$

Again, n_{C_3S} and n_{C_2S} etc. follow from Eq. (11). The A/S ratio can be calculated using Eq. (22). Using the calculated C/S and A/S ratios, the formation of C_4AH_{13} can be examined by substituting the C/S and A/S ratios in C-S-H into Eq. (26). If the A/S ratio exceeds the range defined by Eq. (26), C_4AH_{13} is formed and Case 2 is followed.

In this second case, Case 2, there is adequate A in the slag and C_4AH_{13} is formed. Thus Eq. (26) is used with $n_{CH}^{c} = 0$, giving:

$$\overline{C/S} = \frac{1.8(n_{C_3S} + n_{C_2S}) + n_C^* + 0.85n_S - 4n_A^*}{1.36n_S + n_{C_3S} + n_{C_2S}} \tag{34}$$

in which n_{C_3S} and n_{C_2S} etc. follow from Eq. (11). The A/S ratio in the hydration product C-S-H follows from Eq. (26) and the quantity of the hydration product C_4AH_{13} follows from Eq. (27).

In this model, because no CH from the calcium silicate hydrations is assumed to enter the slag hydration, the Portland cement and slag react independently and only their hydration products C-S-H are equilibrated. Therefore, this model corresponds to the lowest state of CH consumption in the system ($n_{CH}^{c} = 0$).

Model 2: CH enters C-S-H from the slag hydration to sustain a C/S ratio 1.8

In this model, CH from the calcium silicate hydrations is assumed to enter the slag hydration to sustain C/S = 1.8 in the hydration product C-S-H. This C/S ratio was observed in the C-S-H from the Portland cement hydration [10]. It was also in line with the values used in other literature [8]. With increasing slag proportions in the blended cement, the quantity of CH for sustaining the constant C/S ratio in C-S-H also increases. At a certain proportion all the CH will be consumed. After the complete consumption of CH, the C/S ratio diminishes with increasing slag proportions. Therefore, the discussion is divided into two states, corresponding to the partial or complete CH consumption by the slag hydration, respectively.

In the first state, namely State 1, part of CH from the clinker hydration is consumed by the slag hydration. In this state there is still some free CH present in the cement paste. Based on the model assumption, now the C/S ratio in the hydration product C-S-H is 1.8.

Two cases are distinguished depending on the formation of C_4AH_{13} from the slag hydration or not. In Case 1, the A content in the slag is not adequate to obtain the maximum degree of substitution in C-S-H. Hence, C_4AH_{13} is not formed. Now, $\overline{C/S} = 1.8$. Substituting $\overline{C/S}$ into Eq. (25) gives:

$$1.8 = \frac{1.8(n_{C_3S} + n_{C_2S}) + n_C^* + n_{CH}^{c}}{n_{C_3S} + n_{C_2S} + n_S} \tag{35}$$

Solving Eq. (35) gives n_{CH}^{c} as:

$$n_{CH}^{c} = -n_{C}^{*} + 1.8n_{S} \tag{36}$$

A transitional slag proportion, namely λ^0, is defined as the slag proportion at which all the CH is consumed ($n_{CH}^{c} = n_{CH}^{p}$). The transitional slag proportion is solved using Eqs. (14) and (36) as:

$$\lambda^0 = \frac{1.2y_{C_3S} + 0.2y_{C_2S}}{1.2y_{C_3S} + 0.2y_{C_2S} + \gamma \cdot (-y_{C}^{*} + 1.8y_{S,sl})} \tag{37}$$

Therefore, the transitional slag proportion depends on the compositions of clinker and slag, and the slag hydration degree in the paste.

In Case 2, C_4AH_{13} is formed. According to the model assumption, $\overline{C/S} = 1.8$. From Eq. (29) it follows that:

$$1.8 = \frac{1.8(n_{C_3S} + n_{C_2S}) + n_{C}^{*} + n_{CH}^{c} + 0.85n_{S} - 4n_{A}^{*}}{1.36n_{S} + n_{C_3S} + n_{C_2S}} \tag{38}$$

and n_{CH}^{c} is solved as

$$n_{CH}^{c} = -n_{C}^{*} + 1.61n_{S} + 4n_{A}^{*} \tag{39}$$

If all the CH produced by the clinker hydration is consumed by the slag hydration, $n_{CH}^{c} = n_{CH}^{p}$. The transitional slag proportion for Case 2 is calculated from Eqs. (14) and (39) as:

$$\lambda^0 = \frac{1.2y_{C_3S} + 0.2y_{C_2S}}{1.2y_{C_3S} + 0.2y_{C_2S} + \gamma \cdot (-y_{C}^{*} + 1.61y_{S,sl} + 4y_{A}^{*})} \tag{40}$$

At slag proportions higher than λ^0, the amount of CH produced by the hydration of clinker is not sufficient to supply the constant C/S ratio of 1.8 in C-S-H. It is thus all consumed if $\lambda \geq \lambda^0$, resulting in the second state, State 2.

The slag proportion in the blended cement exceeds $\lambda^0 (\lambda \geq \lambda^0)$ in State 2. The slag hydration consumes all CH produced by the clinker hydration, indicating $n_{CH}^{c} = n_{CH}^{p}$. The C/S ratio in C-S-H is lower than 1.8 and is yet unknown. Depending on the formation of C_4AH_{13}, two cases prevail. In Case 1, in which C_4AH_{13} is not formed, the C/S ratio is calculated from Eqs. (14) and (25) as:

$$\overline{C/S} = \frac{3n_{C_3S} + 2n_{C_2S} + n_{C}^{*}}{n_{C_3S} + n_{C_2S} + n_{S}} \tag{41}$$

Note that in Eq. (41), the C/S ratio in C-S-H is completely determined by the entire C contents (excluding those contained in the ettringite) and the entire S contents in the calcium silicates (from clinker) and in the slag. The A/S ratio in C-S-H from the slag hydration is calculated from Eq. (22).

In Case 2, the maximum degree of A substitution is achieved. Substituting Eq. (14) into Eq. (29), the C/S ratio in the hydration product C-S-H reads:

$$\overline{C/S} = \frac{(3n_{C_3S} + 2n_{C_2S}) + n_{C}^{*} + 0.85n_{S} - 4n_{A}^{*}}{n_{C_3S} + n_{C_2S} + 1.36n_{S}} \tag{42}$$

In the equation above, when $\lambda = 1$, it results in the equation in the reaction model for pure slags [7]. The A/S ratio in C-S-H from the slag hydration follows from Eq. (26) and mole of C_4AH_{13} ($n_{AH,sl}$) follows from Eq. (27) from the C/S ratio from Eq. (42).

In this model, because all the CH is available for maintaining a C/S ratio of 1.8 in C-S-H, it is in fact the model with the highest degree of CH consumption by the slag hydration.

Model 3: Part of the CH enters C-S-H from the slag hydration

In many experiments the C/S ratio in C-S-H was found already diminishing even when there was still some free CH prevailing [10, 14, 26, 27]. Model 2 does not account for this limited degree of CH consumption. Hence, another model is proposed (Model 3), in which all CH produced by the calcium silicates is assumed to be available for the slag hydration, but the quantity of CH entering the slag hydration is not sufficient to sustain a constant C/S ratio of 1.8 in the hydration product C-S-H.

First, define the proportion of the consumed CH to the total amount produced, namely p, as:

$$p = \frac{n_{CH}^{c}}{n_{CH}^{p}} \tag{43}$$

whereby $0 \leq p \leq 1$. Furthermore, the C/S ratio of C-S-H formed by the slag hydration cannot exceed the ratio in C-S-H from clinker hydration (1.8, as used in this study). Hence, inequality (31) or (32) applies, depending on the formation of C_4AH_{13}. Hence:

$$\begin{aligned} n_{CH}^{c} = p \cdot n_{CH}^{p} &\leq 1.8n_{S} - n_{C}^{*} \leq 1.8n_{S} - n_{C}^{*} \\ &+ 4n_{AH,sl} \quad (n_{AH}^{sl} \geq 0) \end{aligned} \tag{44}$$

The right parts of inequality (44) ($1.8n_{S} - n_{C}^{*}$ or $1.8n_{S} - n_{C}^{*} + 4n_{AH,sl}$) are actually the surplus of CH needed for maintaining a C/S ratio of 1.8 in C-S-H

formed by the slag hydration in the two cases. A semi-empirical expression for p is proposed here as:

$$p = \frac{1.8n_S - n_C^*}{n_{CH}^p + 1.8n_S - n_C^*} = \frac{\gamma\lambda(1.8y_{S,sl} - y_C^*)}{(1-\lambda)(1.2y_{C_3S} + 0.2y_{C_2S}) + \gamma\lambda(1.8y_{S,sl} - y_C^*)} \quad (45)$$

The expression for p (Eq. (45)) states that the fraction of CH consumed by the slag hydration (p) is linearly proportional to the surplus S (or equivalently, the shortage of C) in the slag for obtaining a C/S ratio of 1.8 in the C-S-H formed (from the slag hydration alone). In other words, a slag where the molar ratio C/S = 1.8, will not need/consume CH. Other (nonlinear) relations would also conceivable, but in chemical engineering it is a common approach to relate mass transfer linearly to a concentration gradient. Furthermore, by definition p obeys the requirement $0 \le p \le 1$. In what follows it will be seen that using this proposed semi-empirical expression for p results in good agreement with experimental observations.

Inequalities (31) and (32) automatically apply with the defined p. Note that in Eq. (45), if $\lambda = 0$, $p = 0$ (no CH consumption); if $\lambda = 1$, $p = 1$ (full CH consumption); and automatically $0 \le p \le 1$. The quantity of consumed CH by the slag hydration (per unit mass of slag) can be calculated from Eq. (46) as:

$$n_{CH}^c = p \cdot n_{CH}^p = p \cdot (1.2n_{C_3S} + 0.2n_{C_2S}) \quad (46)$$

in which p follows from Eq. (45) and n_{C_3S} and n_{C_2S} follow from Eq. (11). It can be seen from Eq. (46) that the total amount of CH consumed by the slag hydration increases with increasing calcium silicates contents in the clinker, thus the C/S ratio in C-S-H is increased. But the extent of the influence is minor. Even though more CH is produced by the clinker hydration, the proportion consumed by slag hydration is smaller (see Eq. (45)). Hence, the total amount of consumed CH remains approximately the same.

Similarly, two cases exist depending on the formation of C_4AH_{13} or not. In Case 1, C_4AH_{13} is not formed. The C/S ratio in C-S-H follows from Eq. (25) using n_{CH}^c from Eq. (46). The A/S ratio is calculated from Eq. (22). The results of Case 1 (C/S and A/S ratios) are always substituted into Eq. (26) to determine the formation of C_4AH_{13}. In Case 2, C_4AH_{13} is formed. The C/S ratio in C-S-H follows from Eq. (29) using n_{CH}^c from Eq. (46). The A/S ratio and quantity of C_4AH_{13} are calculated from Eqs. (26) and (27).

With the three reaction models proposed, quantities and compositions of the hydration products can be calculated from the oxide compositions of starting materials and the slag proportion in the blended cement. With these information, some characteristics of the microstructure of hydrating slag-blended cement paste can be predicted.

Microstructure of hydrating slag cement paste

Molar fractions of hydration products

Molar fractions of the hydration products (C-S-H, hydrotalcite, ettringite etc.) in the hydrating slag cement paste can be calculated by using the stoichiometry models proposed in the previous sections. In the hydrating cement paste, the other two clinker phases (aluminate and ferrite) are also reacting and form some hydration products.

The reactions of aluminate are represented by the following equations [21, 22, 24]:

$$C_3A + CH + 12H \rightarrow C_4AH_{13} \quad (47)$$

$$2C_3A + C\bar{C} + CH + 23H \rightarrow 2C_4A\bar{C}_{0.5}H_{12} \quad (48)$$

$$C_3A + 3C\bar{S}H_2 + 26H \rightarrow C_6A\bar{S}_3H_{32} \quad (49)$$

in which full carbonation of monosulfate (an intermediate product from the reaction of C_3A with sulfate) takes place. In real hydrating cement pastes, ettringite is firstly formed from C_3A and gypsum. Then, it is converted into monosulfate. However, the monosulfate is not commonly observed in mature cement pastes. In a recent work of Brouwers [21, 22, 24], the absence of monosulfate in cement pastes was found to be caused by carbonation. The carbonation effect finally converts the monosulfate into ettringite and hemicarbonate or monocarbonate. Therefore, in this study, the formation of ettringite from C_3A is considered. The remaining C_3A reacts with the CH to C_4AH_{13}. Quantities of ettringite (n_{AFt}^p), monocarbonate (n_{monoc}) and C_4AH_{13} (n_{AH}^p) from the hydration of Portland cement can be appropriated by using the following equations, respectively [21, 22, 24].

$$n_{AFt}^p = n_{gyp}/3 \quad (50)$$

$$n_{AH}^p = n_{C_3A} - 2/3n_{gyp} \quad (51)$$

$$n_{monoc}^p = n_{gyp}/3 \quad (52)$$

The hydration of ferrite is not well understood until now. In this study, the reaction of ferrite follows from the work of Brouwers [21, 22, 24] as:

$$C_4AF + 2C_2S + 10H \rightarrow C_6AFS_2H_8 + 2CH \quad (53)$$

in which the $C_6AFS_2H_8$ is a Fe-containing hydrogarnet phase with 8 OH^- replaced by 2 SiO_4^{4-}. Obviously, the quantity of $C_6AFS_2H_8$ (n_{HG}) equals to the moles of C_4AF (n_{C_4AF}). It must be noted that in real clinker the composition of C_4AF can vary in a range, thus in Eq. (53) the stoichiometry of C_4AF is assumed to be valid for all clinkers. The equation can be used as an approximation to the actual reaction. In the work of Brouwers [21, 22, 24], C_4AF can react with both C_3S and C_2S. Only the reaction of C_4AF with C_2S is here listed because the adoption of C_3S or C_2S does not significantly change the model. The quantity of hydrogarnet equals to n_{C_4AF} according to the reaction equation (53). The quantities of all products present in the hydrating cement paste can be calculated with Eqs. (50)–(53) and the stoichiometric models.

Water retention

When the quantities of all hydration products from the slag and Portland cement hydrations are known, the water retention by these products can be calculated considering different hydration states.

The water content in the hydration products of slag-blended cement is listed in Table 1 (mole/mole product), part of which is taken from Table 1 in Part I of this research [7]. The water-binding characteristic of C-S-H is complex. It is still subject of many researches. This complexity is especially true when considering the effects of varying the C/S ratios in the C-S-H, which applies in the blended cement pastes with different slag proportions. If dried at 105 °C in a carbonation-free environment, for C-S-H with low C/S ratios (1.0–1.1), H/S ratios between 1 and 1.33 were measured [28], while with C/S = 1.22, Lu et al. [29] obtained the H/S ratio 0.50 at the age of 60 days in D-dried state. In the mature C_3S paste in the D-dried state, H/S ratios in C-S-H ranging between 0.97 and 1.24 were measured with the C/S varying from 1.34 to 1.60 [30], which is in good agreement with the experiment of Thomas et al. [31]. Thus, it might be concluded that the water retained in C-S-H at 105 °C (or in the D-dried state) is loosely correlated to its C/S ratio and might be closer to a constant value. In this study, this constant value is fixed as 1.2 and is valid for all C-S-H with different C/S ratios. The water retention at 105 °C (or in the D-dried state) is generally considered to be the ''non-evaporable'' water (see Part I of this study). The water content on a molar basis for C-S-H at 80% RH and in the saturated state is taken from the work of Brouwers [21, 22, 24] as H/S = C/S + 0.8 and H/S = C/S + 1.5, respectively.

Table 1 Water content in the hydration products (column headings indicate the hydration states that the pastes are subject to)

Hydration product	105 °C	80% RH	100% RH
C-S-H	1.2	C/S + 0.8	C/S + 1.5
M_5AH_{13}	7	13	19
C_4AH_{13}	7	13	19
$C_4A\bar{C}_{0.5}H_{12}$	7	12	12
$C_6A\bar{S}_3H_{32}$	8	32	32
$C_6AFS_2H_8$	8	8	18
CH	1	1	1

The total water retained by the hydration products is calculated as

$$n_H = \sum (H_i \cdot n_i) \quad (54)$$

where n_H is the water retained by the hydration product; H_i is the water content in each hydration product, which is taken from Table 1; n_i is the quantity of such hydration product calculated using the proposed models. The water retained at 105 °C (or after being D-dried) is generally designated as the non-evaporable water and its amount reads m_{new} in this study for convenience.

Chemical shrinkage

Similarly, chemical shrinkages of the slag-blended cements are predicted by using the physical properties of the hydration products (Table 2). The physical properties of C-S-H, whose composition varies over a wide range, might vary with various C/S ratios. In this study, the physical properties of C-S-H with various C/S ratios and in the saturated state are calculated using the model proposed by Brouwers [21, 22, 24]. The density of C-S-H is calculated as

$$\rho_{C-S-H} = \frac{87.12 + 74.10\ C/S}{38.42 + 33.05\ C/S} \quad (55)$$

and the molar volume of C-S-H is calculated as:

$$\omega_{C-S-H} = M_{C-S-H}/\rho_{C-S-H} \quad (56)$$

in which the molar mass of C-S-H ($M_{C\text{-}S\text{-}H}$) can readily be calculated from its compositions. Chemical shrinkage is calculated as:

Table 2 Physical properties of hydration products of slag-blended cement in the saturated state

Substance	M (g/mol)	ρ (g/cm^3)	ω (cm^3/mol)
C-S-H	various	various	various
M_5AH_{13}	645.5	1.80	358.12
C_4AH_{13}	668.4	1.80	371.33
$C_4A\bar{C}_{0.5}H_{12}$	564.5	1.98	284.54
$C_6A\bar{S}_3H_{32}$	1255.3	1.78	707.04
$C_6AFS_2H_8$	1042.4	2.24	465.38
CH	74.1	2.24	33.05

$$\Psi = \frac{(V_p + V_{sl}^r + V_H) - V_{hp}}{m} = \frac{(m_p/\rho_p + m_{sl}\cdot\gamma/\rho_{sl} + n_H\cdot\omega_H) - \sum n_i\cdot\omega_i}{m_{sl}+m_p} \quad (57)$$

in which V_p, V_{sl}^r, V_H, V_{hp} are the volumes of Portland cement, reacted slag, retained water and hydration products; i is the hydration products, respectively.

Porosity

Powers and Brownyard [32] developed a general model for describing the structure of hardened Portland cement paste (hcp). In this model, the hcp is generalized to comprise three components, viz. the unreacted cement, hydration products and capillary pores. These concepts apply to the hydrating slag-blended cement as well. Quantities of these components can be mathematically predicted considering the curing conditions and recipes of the pastes with the hydration models proposed in this study. Hence, the model proposed by Powers and Brownyard [32] is further developed for hydrating slag-blended cement paste. The procedure is described below.

The total volume of paste reads:

$$V_{hcp} = m\cdot[1/\rho_c + (w/c)/\rho_w] \quad (58)$$

in which ρ_c is the density of the binder (slag-blended cement) (g/cm^3); ρ_w is density of pore water in the fresh paste, assumed to be 1 g/cm^3; and w/c is the water/cement ratio in mass. ρ_c is calculated from the volumes of Portland cement and slag as:

$$\rho_c = \frac{1}{(1-\lambda)/\rho_p + \lambda/\rho_{sl}} = \frac{\rho_p\cdot\rho_{sl}}{(1-\lambda)\cdot\rho_{sl} + \lambda\cdot\rho_p} \quad (59)$$

in which ρ_p is the density of Portland cement, assumed to be 3.2 g/cm^3 and ρ_{sl} is the specific volume of slag, assumed to be 2.92 cm^3/g.

Complete hydration of Portland cement is assumed to always occur, rendering the hydration degree of slag in the paste as the uncertainty. As observed in experiments, all clinker in the blended cement has hydrated after about one year curing, while the hydration degree of slag can vary in a range.

The paste is assumed to be cured in the saturated state, and all the capillary pores are thus permeable to external water. In other words, all the capillary pores are filled with water. Influences of autogenous shrinkage and drying shrinkage on the apparent volume of the paste are eliminated. The volume of capillary pores thus equals to the difference between the volume of the starting slurry and that of the solids in the hydrating paste, comprising the volumes of the unreacted water and the chemical shrinkage. The volume of the capillary pores (V_{cp}) are calculated as:

$$V_{cp} = V_{hcp} - V_{hp} - V_{sl}^{ur} = m\cdot[1/\rho_c + (w/c)/\rho_w] - \sum n_i\omega_i - m_{sl}\cdot(1-\gamma)/\rho_{sl} \quad (60)$$

in which V_{sl}^{ur} is the volume of unreacted slag and ω_i is the molar volume of hydration product i. The porosity of C-S-H is calculated as:

$$\Phi_{C-S-H} = \frac{32.44}{94.60 + 33.05\ (\overline{C/S} - 1.7)} \quad (61)$$

If all and only the pores in the gel product C-S-H are considered as gel pores (as explained in Part I of this study), the volume of gel pores (V_{gp}) reads:

$$V_{gp} = V_{C-S-H}\cdot\Phi_{C-S-H} = n_{C-S-H}\cdot\omega_{C-S-H}\cdot\Phi_{C-S-H} \quad (62)$$

The capillary and gel porosities of the paste are calculated, respectively, as:

$$\Phi_{cp} = V_{cp}/V_{hcp}; \quad \Phi_{gp} = V_{gp}/V_{hcp} \quad (63)$$

And the total porosity of the hardened cement paste reads

$$\Phi = \Phi_{gp} + \Phi_{cp} \quad (64)$$

The porosity of hydrating slag-blended cement paste depends on many factors, for example the hydration degree of ingredients, the slag proportion in cement, the initial w/c ratio and the hydration state of the samples. The influences of these factors are addressed in the following sections.

Experimental validation of the hydration models and discussions

Six blended cements are selected from literature to validate the proposed models. The oxide compositions of the Portland cements in the blended cements are listed in Table 3. Only the Bogue composition the Portland cement in Cement 4 is given in the literature. Hence, its oxide composition is calculated from its Bogue composition. The mass fractions of the four major clinker phases in the Portland cements are listed in Table 4 after being normalized to a total of 100%. The mineralogical compositions of Cement 1–3, 5 and 6 are calculated using the Bogue's equations. The oxide compositions of slags in the selected blended cements are listed in Table 5, also after being normalized to a total of 100%.

Cement 1 originates from the study of Richardson and Groves [10]. The microstructures and compositions of a group of hardened cement pastes with different slag proportions were analyzed using the TEM with microanalysis combined with EMPA. The slag proportions increased from 0% to 100% divided into nine different degrees. The w/c ratio of the blended cement pastes was 0.4. The pastes were cured up to three years in sealed plastic tube at 20 °C. Both the C/S and A/C ratios in the hydration product C-S-H were measured at 14 months (Table 6).

Cement 2 originates from the study of Taylor et al. [26]. Blended cement paste was made with 59% clinker, 39% slag and 2% gypsum (in mass percentages). The blended cement was mixed with deionized water at a w/c ratio of 0.5 and was sealed into polyethylene vials. The samples were cured at 20 °C for up to

Table 3 Oxide compositions of Portland cement in blended cements

Oxide	Cement 1	Cement 2	Cement 3	Cement 4	Cement 5	Cement 6
C	66.5	68.8	66.0	70.8	67.1	64.8
S	20.2	21.5	21.3	26.9	21.4	22.9
A	6.2	4.9	5.6	1.9	6.1	5.3
M	1.3	1.8	1.2	0	1.6	2.5
$\bar{S}$	2.7	1.2	2.7	0	0.9	1.8
F	3.1	1.8	3.2	0.4	2.9	2.7
Total	100	100	100	100	100	100

Cement 1 originates from the work of Richardson and Groves [10]; Cement 2 from Taylor and Mohan [26]; Cement 3 from Harrisson et al. [13]; Cement 4 from Richardson [27]; Cement 5 from Schäfer [33]; and Cement 6 from Mills [34]. Minor compositions are omitted and the mass percentages are normalized to a total of 100%. The compositions of Portland cement in Cement 4 are calculated from the mass fractions of clinker phases. Free lime content exists in neglectable amount except in Cement 2 with the mass fraction of 0.5%

Table 4 Mineral compositions of Portland cement clinkers in Portland cement in the blended cements

Phase	Cement 1	Cement 2	Cement 3	Cement 4	Cement 5	Cement 6
C_3S	67.4	81.4	61.1	70.7	66.5	47.9
C_2S	10.6	2.5	18.7	23.9	12.9	33.7
C_3A	12.1	10.3	9.9	4.3	11.4	10.2
C_4AF	9.9	5.8	10.3	1.1	9.2	8.2
Total	100	100	100	100	100	100

The compositions of Cements 1, 2 and 3 are calculated by using the Bogue equations

Table 5 Oxide compositions of slags in the blended cements

Oxide	Cement 1	Cement 2	Cement 3	Cement 4	Cement 5	Cement 6
C	41.15	44.76	44.56	41.64	44.0	30.72
S	36.72	35.22	35.74	36.95	35.75	33.03
A	10.86	11.19	11.06	12.55	12.45	16.16
M	7.64	8.70	8.62	8.01	7.79	20.09
$\bar{S}$	3.63	0.13	0.02	0.85	0.01	0
Total	100	100	100	100	100	100

Only the oxides involved in the selected hydration products are listed (C, S, A, M and $\bar{S}$) and the mass percentages are normalized to a total of 100%

Table 6 Measured C/S and A/C molar ratios of C-S-H in hardened slag-blended cement paste (Cement 1, w/s = 0.4, 20 °C, 14 months, after Richardson and Groves [10].

% GGBFS	C/S	A/C
0	1.76	0.027
10	1.89	0.020
25	1.78	0.032
50	1.55	0.050
66.7	1.43	0.065
75	1.37	0.065
83.3	1.38	0.075
90	1.28	0.075
100	1.14	0.095

540 days. The blended cement pastes were studied by using XRD, analytical electron microscopy (AEM) and thermogravimetry (TG). Partial replacement of clinker by slag was found to decrease both the amount of CH existing in the cement paste and the mean C/S ratio of C-S-H.

Cement 3 originates from the study of Harrisson et al. [13]. Pastes of blended cement containing 40% slag were examined using SEM fitted with an energy dispersive X-ray (EDX) system. The pastes were prepared by hand mixing at a w/c ratio of 0.5 and cured at 25 °C for 14 months. After the first two days, the sample was cured in sealed polyethylene containers in water. The observations were similar to those of Taylor et al. [26]: the CH content was reduced by the addition of slag into Portland cement and also the C/S ratio of the C-S-H formed from the clinker hydration decreased. None of the individual phases in the blended cement pastes showed significant compositional variation over time in the period from 28 days to 14 months.

Cement 4 originates from the study of Richardson [27]. Water-activated white Portland cement/slag blend pastes with a w/c ratio of 0.4 were investigated using solid-state ^{29}Si-NMR spectroscopy and analytical TEM. The blends had two slag proportions, 50% and 90% (in mass), respectively. The samples were cured at 25 °C in sealed plastic tubes. C/S and A/S ratios in C-S-H were measured using both NMR and TEM. The test age was unknown. Aluminum substitution for silicon was found in C-S-H.

Cement 5 originates from the study of Schäfer [33]. Cement paste samples were made with a w/c ratio of 0.5 and cured up to one year with different slag proportions. The CH contents of the samples were determined by using a TGA technique with the weight difference in the range between 450 °C and 600 °C, in which the decomposition of the CH takes place. The measurements were further corrected for the weight loss of C-S-H. The amount of CH consumed by the slag hydration can thus be obtained by comparing the amount of CH in the slag cement pastes to that in pure Portland cement pastes. Together with the hydration degrees of slag in the samples, the extent of CH consumption by the slag hydration can be calculated.

Cement 6 originates from the study of Mills [34]. Slag cement paste samples were made with a w/c ratio of 4, and containing different proportions of slag (from 0% to 90% by mass) in the blended cements. The chemical shrinkage was determined by the mass increment of water needed to keep the pyknometer bottles filled to the mark. The amount of m_{new} was determined by first drying the slurry samples at 110 °C and then igniting them at 1,050 °C. The measurements continued for about 3 years.

Composition of C-S-H

First, the three models are employed to model the hydration of Cement 1. The hydration degrees of slag and Portland cement in the paste must be determined before the modeling process. To the authors' knowledge, until now general models for determining the hydration degrees of slag and Portland cement in the blended cement paste at given ages are not available, yet. The hydration degree can be influenced by many factors, such as the curing conditions, test ages, w/s ratios, slag proportions and probably the most important one, the slag reactivity. A tentative degree of 70% ($\gamma = 0.7$) for the slag hydration and complete hydration of Portland cement is assumed in this study. This hydration degree is further assumed to be valid for all slag proportions. The basic reasons for this assumption are the observations by Hinrichs and Odler [5], Battagin [4] and Lumley et al. [6]. The effect of the slag/clinker ratio on the slag reactivity was found to be quite limited. Only for high slag proportions (from 80% and up) an obvious decline in the slag reactivity was observed. The influence of different slag hydration degrees on the model predictions will also be investigated in later part of this study.

The measured A/C ratios in C-S-H are converted to A/S ratios by using the measured C/S ratios. The compositions of C-S-H predicted by the proposed models are compared to the experimental observations (Fig. 1a, b). It can be seen that the C/S ratios predicted by Model 1 are slightly lower than the measurements in the experiments. The low C/S ratios indicate that the exclusion of CH from the slag hydration decreases the C/S ratios in C-S-H. So, this assumption is unlikely to be true. The A/S ratios predicted by Model 1 at low slag proportions are higher than the measurements. The discrepancy comes from the predicted low C/S

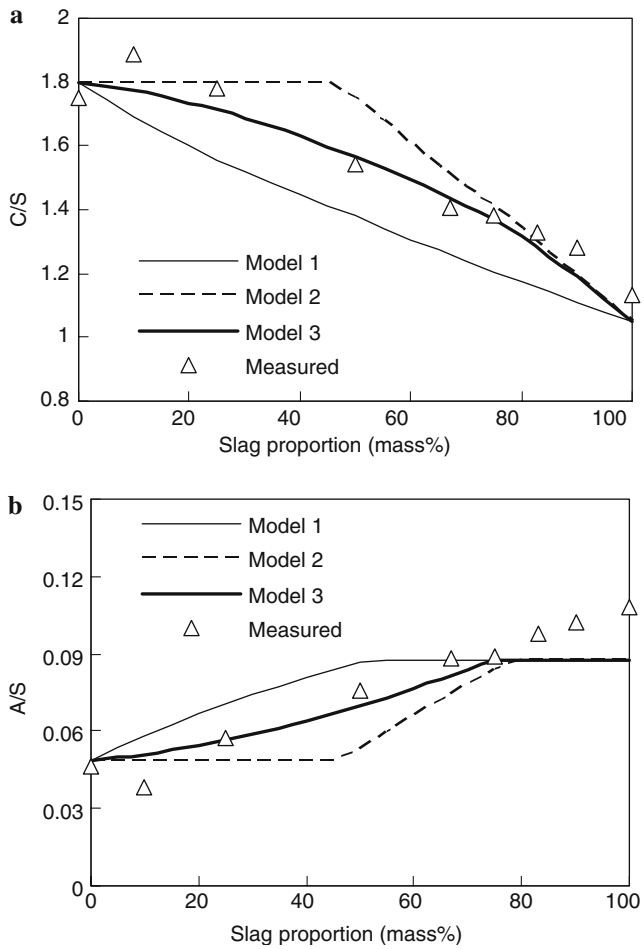

Fig. 1 (**a**) C/S ratio in the hydration product C-S-H: model prediction and comparison with measurement by Richardson and Groves [10]. (**b**) A/S ratio in the hydration product C-S-H: model prediction and comparison with measurement by Richardson and Groves [10]

ratio in C-S-H since C-S-H with a low C/S ratio can structurally incorporate more A, resulting in a higher A substitution degree in the C-S-H (higher A/S ratio).

The C/S ratios predicted with Model 2 accord better with the experimental observations as compared to those with Model 1. Therefore, most likely CH from the Portland cement hydration enters the C-S-H from the slag hydration and increases its C/S ratio. However, the C/S ratios predicted by Model 2 at some slag proportions are slightly higher than the measurements, especially at intermediate proportions, and the predicted A/S ratios are apparently lower than the measurements. The observations in the experiments showed that blending slag with Portland cement at even low slag proportions (25% and 50% as used in the experiments) already lowered the C/S ratios in C-S-H and increased the A/S ratios. This trend was also evident in the experimental results for Cements 2–4. Therefore, the quantity of CH entering the slag hydration can hardly be sufficient to sustain a constant C/S ratio (1.8).

The predictions by Model 3 accords best with the observations. Both the C/S and A/S ratios in C-S-H are well predicted. At slag proportions higher than 60%, the predicted A/S ratios do not increase any further due to the lack of aluminum available to achieve the maximum substitution degree. The A/S ratios are thus governed by the slag composition (see Eq. (22)). In the experiments, the A/S ratio in C-S-H kept increasing at high slag proportions ($\lambda > 60\%$), which are slightly higher than the model predictions. A possible explanation for these higher A/S ratios is the probable intimate mixing of C-S-H and hydrotalcite in the hydration products. In the blended cement pastes with high slag proportions, a significant amount of hydrotalcite is formed and is closely mixed with C-S-H. To analyze the compositions of pure phase C-S-H in these pastes became therefore more difficult. Most likely higher A and M contents in it were measured. Hence, the measurement of the C/S ratios is more reliable and more suitable for validation of the models.

It can be concluded from all experimental results and model predictions that CH produced by the Portland cement hydration is most likely to be available for the slag hydration. It enters the slag hydration to increase the C/S ratio in C-S-H compared to that of the anhydrous slag.

The three hydration models are also employed to model the hydration of the other three blended cements. The predicted compositions of C-S-H are compared to the measurements in experiments (Fig. 2a, b). Similar conclusions can be drawn. The compositions predicted by these models accord well with the experimental observations. Among these models, Model 3 generally gives the best predictions for the composition of the main hydration product, C-S-H, especially for its C/S ratio.

Model 3 is thus recommended for modeling the hydration of the slag-blended cement since it consistently gives the best predictions for all cements under investigation. It is also used in the following discussions.

The influence of slag hydration degree (γ) on the prediction of the composition of C-S-H is further investigated. To this end, Model 3 is again used and is applied to Cement 1. Although the hydration degrees of slag are assumed to vary over a wide range (0.5–1), this variation has only a very minor influence on the predicted composition of C-S-H (Fig. 3a, b). This is especially true when considering the C/S ratio in C-S-H. The influence of slag hydration degree on the compositions of C-S-H is more prominent at intermediate slag

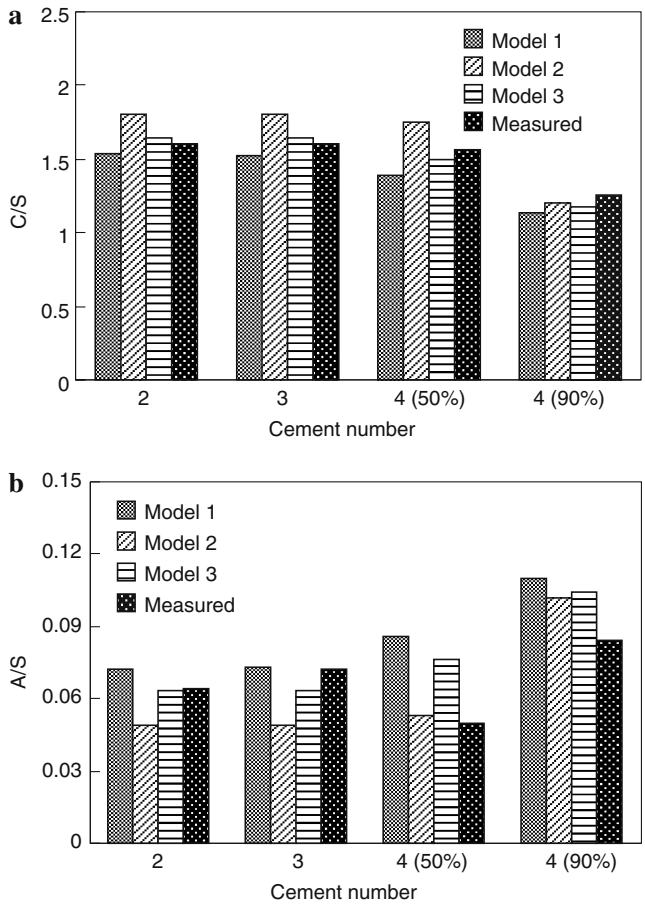

Fig. 2 (**a**) C/S ratio in the hydration product C-S-H: predicted from Cements 2 to 4 and comparison with measurements by Taylor and Mohan [26], Harrisson et al. [13], and Richardson [27]. (**b**) A/S ratio in the hydration product C-S-H: predicted from Cements 2–4 and comparison with measurements by Taylor and Mohan [26], Harrisson et al. [13], and Richardson [27]

proportions. But even so, the variation of C/S ratios at 50% slag (in mass percentage) is within the range of 5.2% using the measured values in experiments as standard, which is probably less than the errors involved in the experimental data for C/S ratios. Therefore Model 3 proposed in this study is not sensitive to the hydration degree of slag in the pastes. It can be used for computing the composition of C-S-H, even if the hydration degree of slag is not completely clear.

In Fig. 4, the relationship between the compositions of C-S-H (the S/C and A/C ratios) is examined by using the experimental measurements. The A/C and S/C ratios in C-S-H from Cements 2–4 are generally consistent with the relation proposed by Richardson [18] (Eq. (7), included in the figure as well).

CH consumption

The proportion of CH consumed by the slag hydration is an important feature of the hydration models proposed in this research. In this section, the proposed expressions for the amount and proportion of CH consumed by the slag hydration are validated with measurements in experiments using Cement 5. The validations are based on Model 3 because this model provides the best agreements and is therefore recommended for modeling the hydration of blended cement.

The amount of CH consumed by slag hydration is calculated by using the semi-empirical equations (Eqs. (43)–(46)) in Model 3. It is further validated with the measurements by Schäfer [33]. They are calculated at different slag proportions and are plotted in Fig. 5a, together with the measured values in the experiments. The influence of varying the degrees of slag hydration is also included. It can be seen that the proportion of CH entering the slag hydration increases with increasing slag proportions in the blended cement. This is also true while increasing the hydration degree of slag, since the net consequence is also to increase the quantity of hydrated slag. Both the predicted and measured amounts of CH consumed by the slag hydration are plotted in Fig. 5b. For 40% and 80% of slag in the blended cement, the measurements are within the range of the predictions. For the blends with 20% slag, the prediction is slightly higher than the

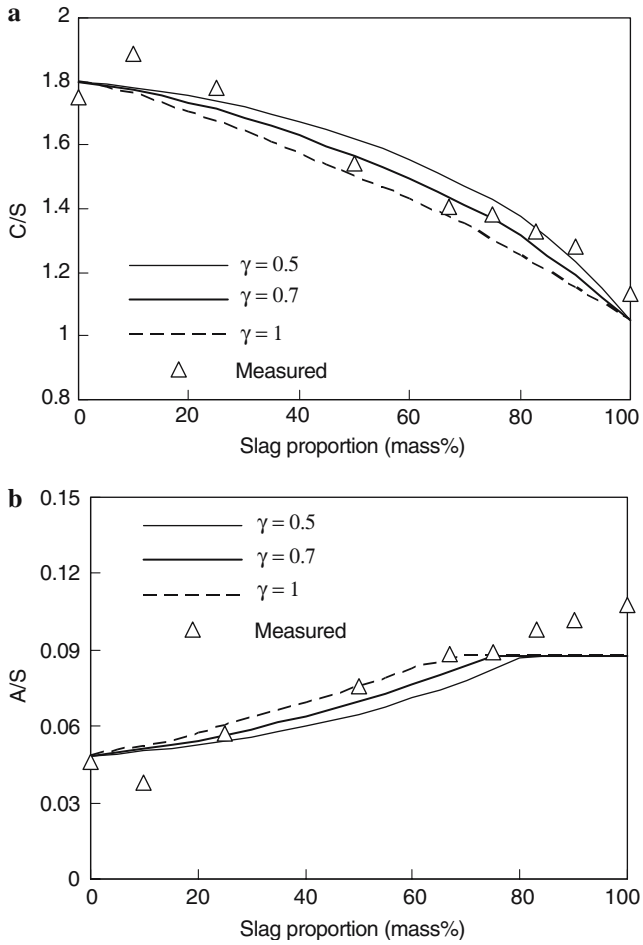

Fig. 3 (**a**) Effect of slag hydration degree on the C/S ratio in C-S-H: Computed with Model 3 and Cement 1. (**b**) Effect of slag hydration degree on the A/S ratio in C-S-H: Computed with Model 3 and Cement 1

measurement due to the higher prediction of proportion on CH consumption in the Model 3 (see Fig. 5a). As a total, the model predictions are in good agreement with the measurements, which proves that the use of Eq. (45) is appropriate for predicting the fraction of CH consumed by slag hydration.

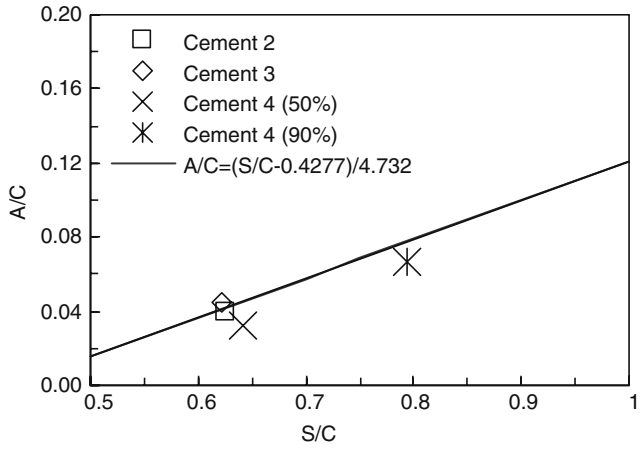

Fig. 4 The S/C and A/C ratios in C-S-H from Cements 2 to 4, and comparison with the relation by Richardson [18]

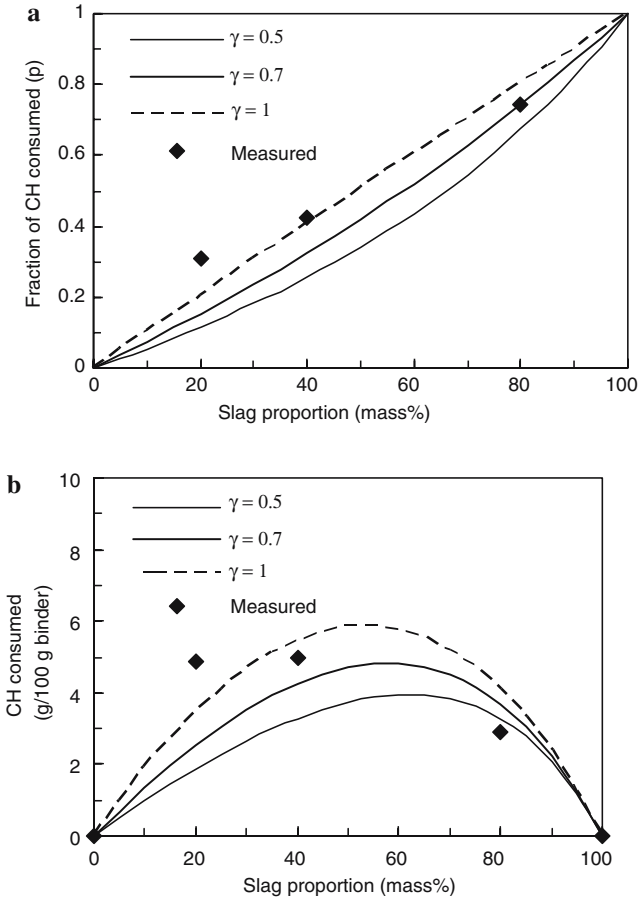

Fig. 5 (**a**) Predicted and measured proportion of CH entering the slag hydration (γ = 0.5, 0.7, 1, predicted with Cement 5, Model 3). Measurements are taken from the experimental data by Schäfer [33]. (**b**) Predicted and measured amount of CH consumed by the slag hydration (γ = 0.5, 0.7, 1, Predicted with Cement 5, Model 3). Measurements are taken from the experimental data by Schäfer [33]

Molar fractions of hydration products

The calculated molar fractions of hydration products versus the slag proportions are plotted in Fig. 6a, taking Cement 1 as example and again using Model 3. The relative hydration degree of slag is 0.7. Clearly, C-S-H is the most abundant product at all slag proportions. With increasing slag proportions in the blended cement pastes, the amount of C-S-H also increases substantially. Meanwhile, the quantity of CH decreases, becoming very low when $\lambda = 0.8$. The quantities of hydrotalcite and ettringite increase with the slag proportions in the cement due to the quantity of slag from which they are formed. The proportion of C_4AH_{13}

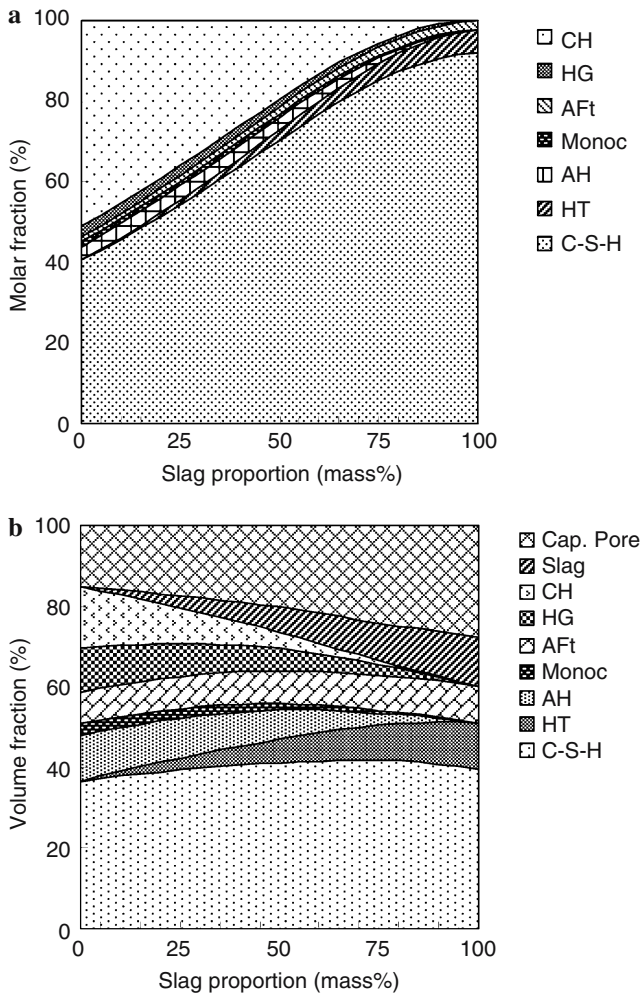

Fig. 6 (**a**) Molar fractions of hydration products in hydrating slag-blended cement paste. Predicted with Model 3, Cement 1. Hydration degree of slag is 0.7 and Portland cement has completely hydrated. (**b**) Volume fractions of hydration products and other phases in hydrating slag-blended cement paste. Predicted with Model 3, Cement 1, w/c = 0.5. Hydration degree of slag is 0.7 and Portland cement has completely hydrated. Predictions are made assuming the paste is maintained in the saturated state

always remains very low (Case 1). At some proportions it is even entirely absent (Case 2).

The volume fractions of hydration products and other phases (capillary pores and unreacted slag) are predicted with the models and plotted in Fig. 6b. Cement 1 and Model 3 is again used and the relative hydration degree of slag is 0.7. Portland cement has completely hydrated in the prediction. The paste is assumed to be cured in the saturated state. It can be seen that C-S-H is again the dominant phase in the paste in volume for all slag proportions. However, its fraction is approximately constant, about 40% of the paste. The volume fraction of ettringite (AFt) is approximately constant as well, due to the comparable sulfate content in the Portland cement and in the slag. Remarkable reductions of the fractions of CH, C_4AH_{13} and hydrogarnet phases are noticed in the figure with increasing slag proportions. Since these phases are normally formed in crystals and their surfaces can act as channels for gas and liquid transfer in the matrix, it would be expected that pastes made with higher slag proportions will have denser microstructures and are less permeable. This effect is even enhanced by the increasing amount of hydrotalcite, which is normally formed as a inner product and is intimately mixed with C-S-H.

Water retention

The results of experiments carried out by Mills [34] are used for validating the present model predictions on water retention. The retained water in the hydration products of Cement 6 in different hydration states (being heated to 105 °C, equilibrated to 80% RH and 100% RH) is predicted (Fig. 7a–c). Model 3 is used for modeling and different degrees of slag hydration in the blended cements (γ = 0.5, 0.7 and 1) are considered. Increasing the slag proportions in the blended cement is shown in the predictions to have only a mild influence on the level of retained water in the hydration products.

The predicted m_{new} with different slag hydration degrees is plotted in Fig. 8a together with the experimental results. The predictions are in good agreement with the results. The measured values are slight higher than the predictions corresponding to full hydration of slag. The predicted values are also within the range measured by Cesareni and Frigione [35] (0.1–0.22 g/g original cement), and also the trend is in good agreement with their measurements. A sharp decline in m_{new} at high slag proportions (approximately > 80%) was observed by Cesareni and Frigione [35], while a plateau occurs in the model predictions. This discrepancy comes from the assumption that for all slag proportions and at the considered age, the slag hydration degrees are the same, which was shown to be invalid for high slag proportions [5, 6]. Therefore, at high slag proportions, the degree of slag hydration might decrease sharply, yielding a sharp decline in the retained water content. Considering this correction for the slag hydration degree at high slag proportions, a sharp decline can be expected as a consequence.

Chemical shrinkage

Chemical shrinkage of the hydration of Cement 6 is predicted with the hydration models and is plotted in

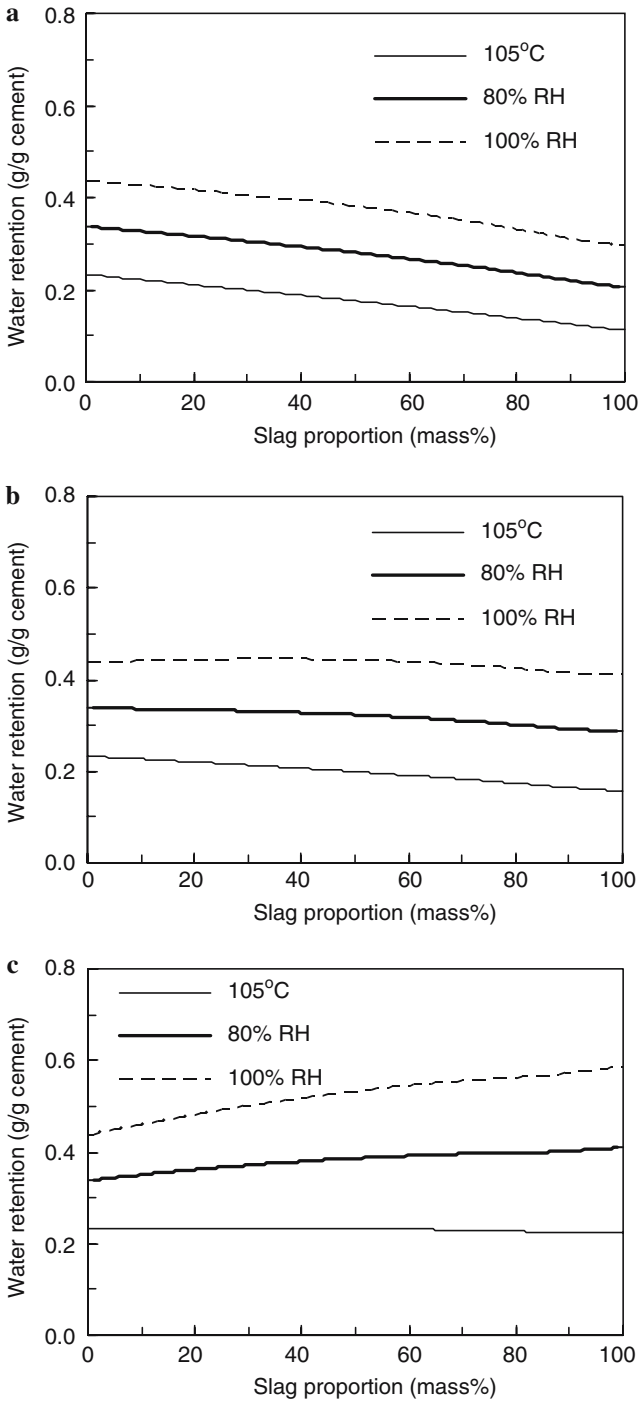

Fig. 7 (**a**) Water retention in the hydration products in different hydration states versus the slag proportion in the blended cement (Cement 6, $\gamma = 0.5$, Model 3). (**b**) Water retention in the hydration products in different hydration states versus the slag proportion in the blended cement (Cement 6, $\gamma = 0.7$, Model 3). (**c**) Water retention in the hydration products in different hydration states versus the slag proportion in the blended cement (Cement 6, $\gamma = 1$, Model 3)

Fig. 8b together with the measured values. Predictions by Model 3 are used with different slag proportions in the cement. One can see that the hydration degree of

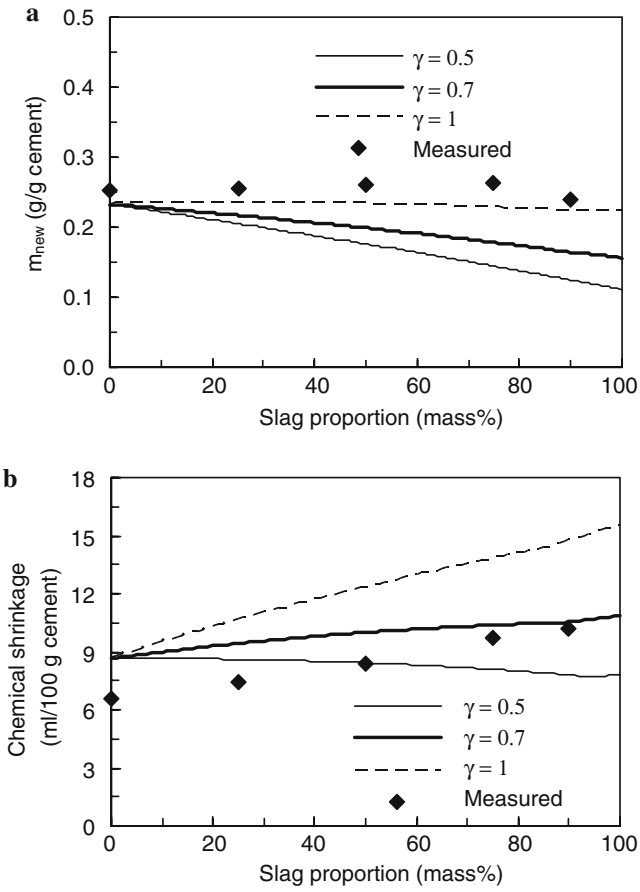

Fig. 8 (**a**) Measured and predicted m_{new} of hydrated slag-blended cement paste (Cement 6, Model 3). Measurements are taken from the experimental data by Mills [34]. (**b**) Measured and predicted chemical shrinkage of hydrated slag-blended cement paste (Cement 6, Model 3). Measurements are taken from the experimental data by Mills [34]

slag in the paste has a dominant influence on the chemical shrinkage of the blended cement, contrary to that on m_{new}. At given ages, higher degrees of slag hydration can be achieved for slags more reactive. Thus, larger chemical shrinkage is expected. For full hydration of reactants, the chemical shrinkage of slag-blended cement hydration (for 50% slag, about 12 ml/100 g cement) is significantly higher than that of pure Portland cement (around 8.7 ml per 100 g cement reacted) (see Fig. 8b for $\lambda = 0$). For slags with medium reactivity, the chemical shrinkage does not differ significantly from that of Portland cement and decreases slightly with increasing slag proportions. For low slag hydration degrees, which are typical for cements high in slag proportions or containing slag of low reactivity, lower chemical shrinkage is expected. The measured values of chemical shrinkage for all slag proportions are slightly lower than the predictions corresponding to a full hydration slag due to the fact that not all the

pores created by the chemical shrinkage of reactions are accessible to external water. However, the trend of the predictions is in good agreement with that shown in the measurements.

Porosity

Porosities of hydrating blended cement pastes are plotted in Fig. 9a–c, taking Cement 1 as example and using Model 3 predictions. The predictions are made with the assumption that the pastes are cured in the saturated state (no drying or autogenous shrinkage) and dried at 105 °C (or after being D-dried), a state in which the water remaining is regarded to be structurally bound in the product.

In Fig. 9a, the porosities are plotted versus the slag proportions in the cement. The hydration degree of slag is assumed to be 0.7 for all proportions and the water cement ratio of the initial paste is 0.5. It can be seen in the figure that with increasing slag proportions in the paste, the total, capillary and gel porosities increase as well. The trends for all three porosities are similar, while the gel porosity increases less prominently. The influence of slag proportions on the porosities as predicted by the hydration model agrees with the observations by Uchikawa et al. [36] and Cesareni and Frigione [35]), especially for gel porosities. A decline at high slag proportions, as observed in experiments, is associated with the low slag hydration degree in cement, which is not accounted for in the prediction. In general, pastes made with slag-blended cement show higher porosities than those made with ordinary Portland cement.

In Fig. 9b, the porosities are plotted versus the hydration degree of slag (γ) in the cement. The proportion of slag (λ) is assumed to be 60% by mass and the water cement ratio of the initial paste (c) is 0.5. Contrary to the influence by slag proportions, the slag hydration degree has more prominent influence on the capillary and gel porosities. The capillary porosity increases with increasing slag hydration degrees, which is reasonable because of the continuous consumption of remaining water in the paste. The increasing gel porosity is associated with the increasing volume of gel products and its high porosity. If more slag has hydrated, more gel product (C-S-H as considered in this study) is produced, which has lower C/S ratio (see Fig. 1a). The porosity of C-S-H with lower C/S ratios is also higher. However, the total porosity keeps almost constant.

The influence of initial w/c of the paste on the porosities is plotted Fig. 9c. The slag proportion is 60% by mass and the hydration degree (γ) is 0.7. Note that in all the calculations the clinker is assumed to hydrate completely. The total and capillary porosities increase dramatically with increasing initial w/c ratios, because of the presence of more free water in the paste. The gel porosity decreases with higher w/c ratios because of the

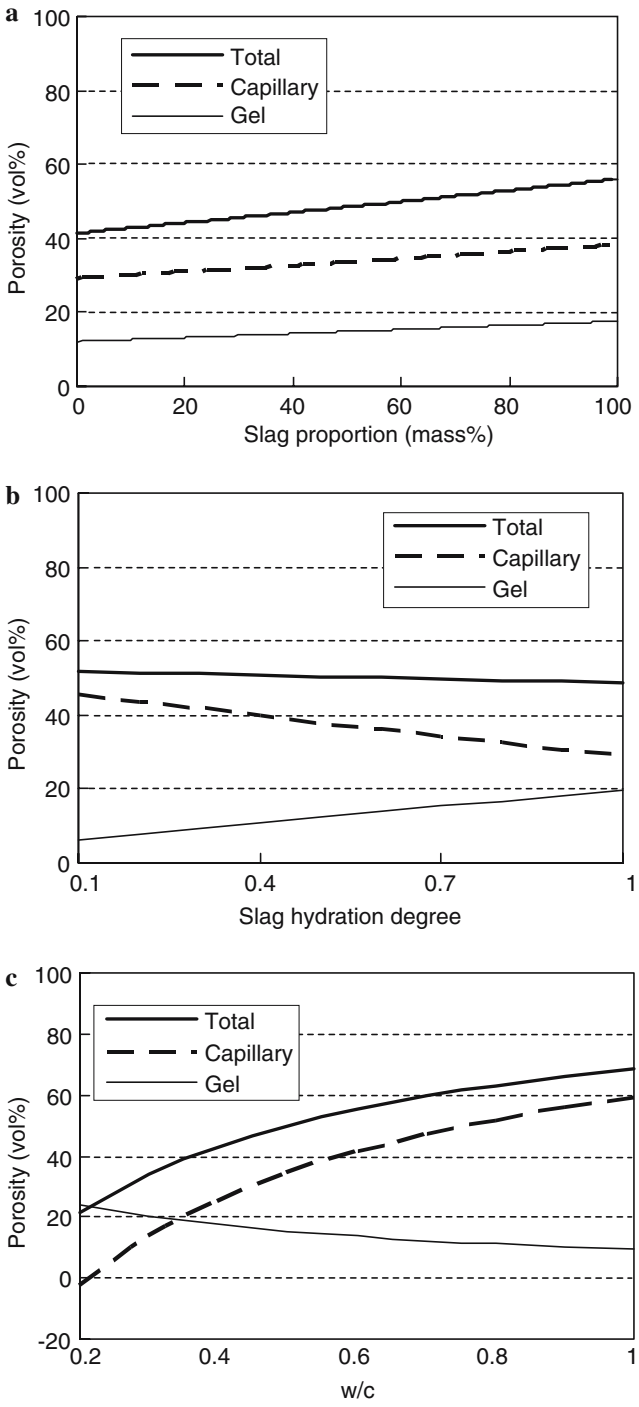

Fig. 9 (**a**) Total, capillary and gel porosities of hydrating slag-blended cement paste versus the slag proportions. (**b**) Total, capillary and gel porosities of hydrating slag-blended cement paste versus the slag hydration degree. (**c**) Total, capillary and gel porosities of hydrating slag-blended cement paste versus the initial w/c ratio

increased volume of the starting pastes. This effect could be partly counteracted by the larger slag hydration degrees with higher w/c ratios. Therefore, the gel porosity would decrease very slightly, or keep almost constant. The trend for the influence of w/c ratios on the porosities is in good agreement with the observations by Cesareni and Frigione [35]. Negative values for low w/c ratios are predicted due to the hydration degrees assumed in the simulation, which can not be achieved because of the limit of space for the growth of products (see Part 1 of this study [7]).

The capillary pores are generally regarded to be responsible for the strength decay and mass transfer in the porous structure. Hence, its volume should normally be minimized. The use of slag in cement does not contribute to the strength and durability of concrete in this respect, because it increases both the total and capillary porosities. However, the capillary porosity is greatly influenced by the reactivity of slag. High slag hydration degree in cement dramatically reduces the capillary porosity, and increase the gel porosity. Hence, the reactivity of slag deserves serious consideration in practice, and should be evaluated before application. The w/c ratio of the recipe is essential in regard to porosities. Denser structures are obtained with lower w/c ratios.

Conclusions

This study proposed and validated three reaction models for the slag-blended cement by quantifying the hydration products and determining the composition of C-S-H, whereby the hydration of calcium silicates in the clinker interacts with the slag hydration. A compositional equilibrium of C-S-H is used in developing the models. Various blending proportions of slag are considered in the models. Three modes of CH consumption by the slag hydration are investigated, resulting in three reaction models. In the models, the degrees of slag and Portland cement hydration are accounted for using a relative slag hydration degree (γ), which can be determined in practice according to the curing condition, age and slag reactivity etc. The Model 3 gives the best accordance with experimental results. The variations in the relative degree of slag hydration show no significant influence on the predictions of models.

Based on the investigations in this research, the conclusion outlined below can be drawn:

1. The main hydration products of slag-blended cement comprise C-S-H, CH, hydrotalcite, ettringite and C_4AH_{13}. C-S-H is the most abundant hydration product. CH is formed from the clinker hydration and interacts with the slag hydration to increase the C/S ratio in C-S-H. The amount of CH entering the slag hydration is related to the blend proportions of slag in the cement.
2. Increasing the slag proportions in the cement increases the proportions of C-S-H in the hydration products. Blending slag with Portland cement clearly lowers the C/S ratio in C-S-H and increases the A/S ratio.
3. The A content in slag is first combined with M to form the hydrotalcite and with $\bar{S}$ to form the ettringite. The remaining A enters C-S-H to substitute for S. If the maximum degree of A substitution is achieved, the remaining A reacts to the AFm phase (C_4AH_{13}).
4. The proposed models can successfully predict the compositions of the hydration products, such as the C/S and A/S ratios in C-S-H, and determine their quantities. Amongst the three models, Model 3 consistently yields the best predictions and its use is thus recommended for modeling the hydration of slag-blended cement. According to this model, the amount of CH consumed is proportional to the difference between C/S ratio of the slag and 1.8.
5. Change of the slag proportions at low or medium levels in the blended cement has only a minor influence on the level of water retained by the hydration products. But the slag-blended cement might exhibit significantly higher chemical shrinkage than Portland cement. The difference in chemical shrinkage between the blended cement and Portland cement can be more prominent if the slag content in the cement is high and/or the slag has high reactivity.
6. The total, capillary and gel porosities increase slightly with slag proportions in the cement. The increase of slag hydration degree reduces the capillary porosity of the paste, but increases its gel porosity. The capillary porosity increases dramatically with w/c ratios. Hence, among various factors affecting the porosities of cement paste, the slag reactivity and w/c ratio deserve special attentions.

Acknowledgements The authors wish to thank the following institutions for their financial support of the present research: Dr. ir. Cornelis Lely Foundation, Delta Marine Consultants, Betoncentrale Twenthe, Rokramix, Dutch Ministry of Infrastructure, SenterNovem Soil+, Jaartsveld Groen en Milieu.

References

1. Lura P (2003) Autogenous deformation and internal curing of concrete. PhD Thesis, Delft University of Technology, Delft, The Netherlands
2. Escalante-García JI, Sharp JH (1998) Cem Con Res 28:1259

3. Luke K, Glasser FP (1988) Cem Con Res 18:495
4. Battagin AF (1992) In: Mullick AK (ed) Proc. 9th ICCC, vol. III. National Council for Cement and Building Materials, New Delhi, India, pp 166–172
5. Hinrichs W, Odler I (1989) Adv Cem Res 2:9
6. Lumley JS, Gollop RS, Moir GK, Taylor HFW (1996) Cem Con Res 26:139
7. Chen W, Brouwers HJH (2005) J Mat Sci (in review)
8. Taylor HFW (1997) Cement chemistry, 2nd edn. Thomas Telford, London, U.K.
9. Regourd M (1980) In: Proc. 7th ICCC, vol. 1, Paris, France, pp III 2/10–2/24
10. Richardson IG, Groves GW (1992) J Mat Sci 27:6204
11. Pietersen HS, Bijen JM (1994) In: Goumans JJJM, van der Sloot HA, Aalbers TG (eds) Environmental aspects of construction with waste materials. Elsevier, Amsterdam London New York Tokyo, pp 949–957
12. Hill J, Sharp JH (2003) Cem Con Comp 24:191
13. Harrisson AM, Winter NB, Taylor HFW (1987) Mat Res Soc Symp Proc 85:213
14. Duchesne J, Bérubé MA (1995) Adv Cem Based Mater 2:43
15. Groves GW, Le Sueur PJ, Sinclair W (1986) J Am Ceram Soc 69:353
16. Macphee DE, Atkins M, Glasser FP (1989) Mat Res Soc Symp Proc 127:475
17. Richardson JM, Biernacki J, Stutzman PE, Bentz DP (2002) J Am Ceram Soc 85:947
18. Richardson IG (2000) Cem Con Comp 22:97
19. Wang S, Scrivener KL (2003) Cem Con Res 33:769
20. Taylor HFW (1993) Adv Cem Bas Mater 1:38
21. Brouwers HJH (2003) In: Fisher HB (ed) Proceedings 15th Ibausil (Internationale Baustofftagung), Weimar, 1-0553-1-0566. F.A. Finger-Institut für Baustoffkunde, Weimar, Germany
22. Brouwers HJH (2004) The work of Powers and Brownyard revisited: composition of Portland cement paste, 2nd edn. CE&M Research Report 2004W-006/CME-001, University of Twente, Enschede, The Netherlands
23. Brouwers HJH (2004) Cem Con Res 34:1697
24. Brouwers HJH (2005) Cem Con Res 35:1922
25. Young JF, Hansen W (1987) Mat Res Soc Symp Proc 235:313
26. Taylor HFW, Mohan K, Moir GK (1985) J Am Ceram Soc 68:685
27. Richardson IG (1997) In: Proc. 10th ICCC, vol. 2, Göthenburg, Sweden, p 2ii068
28. Steinour HH (1947) The System CaO-SiO_2-H_2O and the Hydration of the Calcium Silicates. Bull. 18, Res. Lab. Of Portland Cement Association, by American Chemical Society. Reprinted from Chem Rev 40(3) pp 391–460 (June 1947)
29. Lu P, Sun G, Young JF (1993) J Am Ceram Soc 76:1003
30. Kantro DL, Weise CH, Brunauer S (1966) In: Symposium on structure of Portland cement paste and concrete. Highway Research Board, Special report 90, Washington, U.S., pp 309–327
31. Thomas JJ, Chen JJ, Jennings HM (2003) Chem Mater 15:3813
32. Powers TC, Brownyard TL (1948) Studies of the physical properties of hardened Portland cement paste. Bull. 22, Res. Lab. of Portland Cement Association, Skokie, IL, U.S.A. Rreprinted from J Am Concr Inst (Proc.) 43 (1947) pp 101–132, 249–336, 469–505, 549–602, 669–712, 845–880, 933–992
33. Schäfer E (2004) Einfluss der Reaktionen verschiedener Zementhauptbestandteile auf den Alkalihaushalt der Porenlösung des Zementsteins. PhD Thesis, Technical University of Clausthal, Clausthal, Germany
34. Mills RH (1986) In: Frohnsdorff G (ed) ASTM STP 897, ASTM, Philadelphia, U.S., pp 49–61
35. Cesareni C, Frigione G (1966) In: Symposium on structure of Portland cement paste and concrete. Highway Research Board, Special report 90, Washington, U.S., pp 48–57
36. Uchikawa H, Uchida S, Ogawa K (1986) In: Proc. 8th ICCC, vol. 4, Rio de Janiero, Brazil, pp 251–256